Influence of Cd-doping at electronic and band structure characteristics of gadolinium oxide: A DFT based theoretical study

Sana Wajid[1], Malik Sajjad Mehmood[1, *], Mansoor Ahmad Baluch[2]

[1]University of Engineering and Technology, 47050, Taxila, Pakistan.

[2]Punjab Higher Education Commission, PHEC, Lahore, Pakistan.

***Corresponding Author:** msajjad.82@gmail.com&malik.mehmood@uettaxila.edu.pk

Abstract

The optical uses of Gd_2O_3 have attracted interest in optoelectronics and have increased its popularity in industry. With the use of density functional theory, the SCF, band structure and density of states (DOS) of cubic Gd_2O_3 are examined. For this, Gd_2O_3 supercell has been created with a scaling of (211) and examines the electronic characteristics such as band gap and DOS by using DFT. After this, the effect of Cd doping on the characteristics of Gd_2O_3 nanoparticles is also explored while adding one Cd atom super cellular level of scale (221). The calculations indicate that SCF converges with total energy -689.288 to -1368.33 RY, which suggests that the dopant (Cd) has a substantial impact on the overall structure and electronic properties of the system. After the convergence of SCF, results reveal that both pure Gd2O3 and Cd-doped Gd2O3 were metallic in nature. They were characterized with an extremely small gap or practically negligible small difference between the valence and conduction bands. This indicated that both structures of Gd2O3 are metallic; having overlapped valence and conduction bands.

Keywords: DFT, Gd_2O_3; Cd-doping; Band Structure; Density of States.

Article History: Received: 26th July 2022, **Revised:** 8th June 2023, **Accepted:** 10th June 2023, **Published:** 30th July 2023.

Introduction

Gadolinium oxide (Gd_2O_3) comes in the form of a white, odorless powder that is acid soluble, and is available in both bulk and nanoparticle form [1]. Gadolinium (Gd) is ferromagnetic below its Curie point i.e., 20 °C (68 °F), and has a stronger magnetic field attraction than nickel. Above the Curie temperature, Gd is the element that is most paramagnetic [2]. Due to distinctive structural and electrical characteristics of Gd (because of 4f electrons), its sesquioxides find significant uses in the microelectronic, optoelectronic, and optical device industries [3]. The structural flexibility of rare-earth sesquioxides (including Gd) make them a potential candidate for utilized in solid oxide fuel cells (SOFC) [4, 5] as oxygen-ion conductors [6, 7], oxygen sensors [8], membrane reactors for oxidative catalysis [9], and thick ceramic membranes [5, 10] for oxygen separation [11]. Lanthanide elements and their compounds including Gd_2O_3 are frequently used in several technical fields including electronics, magnetics, optics, biomedicine, and catalytic converters etc. [4, 5, 8].

Gd_2O_3 was generally observed in cubic form [12], considered as an effective compound in antireflective coatings due to its high refractive index. In addition natural form, Gd_2O_3 nanoparticles have gain much attention in recent years because of its unusual magnetic, band structure and optical properties[13]. These nanoparticles may exist in a variety of morphologies, including hollow spheres, nanotubes, nanoplates, nanorods and microrods with improved chemical and thermal stability [14-17]. In addition, it is easy to dope some other additional ions atoms or ions from transition metals and lanthanides to tune its properties with respect to end user applications by using various chemical and physical means including intense lasers and e-beams [18-22]. However, it requires the detail understandings of band structure and optical characteristics [23, 24] of material under investigations.

To get information about structural and optical characteristics Density Functional Theory (DFT) is employed as a powerful theoretical tool. DFT enables the calculation of electronic properties by solving the Kohn-Sham equations, which describe the behavior of non-interacting electrons in an effective potential [25]. The exchange-correlation functional has been utilized for quantifying the electron-electron interactions; and getting

the accurate description of the electronic structure of materials. A few studies have been performed for unrevealing the band structure and other characteristics of Gd_2O_3 while using DFT. In this context, Hermet. J. et. At., [26] has conducted DFT calculations for quantifications of oxidation and hyderation of Gd-doped barium cerate and found that Gd is the most suitable dopdent with both processes i.e. oxidation and hydration are exothermic one with enthalpies -0.70 eV and -1.34 eV, respectively. In another study, Xia X et. Al., [13] has studied the characteristics stability (electronics and magnetic) for cluster of $(Gd_2O_3)n$ for n =1 to 10 using DFT (spin polarized), and found the elongation in Gd-O bonding for increasing the number of clusters. More recently, Lu Y. et al., [9] has conducted first principle calculations for the calculation of optical and band structures of Gd_2O_3 and Fe-doped Gd_2O_3 and found the values 2.60 eV and 0.61 eV, respectively.

In this study, the aim is to investigate the electronic band gap of Gd_2O_3, and the influence in the properties when doping the Cd at super cellular level. The calculations are done while using the local density approximation (LDA) and generalized gradient approximation (GGA) methods with computational details given in subsequent section.

Computational Details

All computations in this study were performed upon by utilizing the CASTEP code in the Materials Studio (MS) 6.1 software based on the Density Functional Theory (DFT) approach. DFT is employed to compute the structural and electronic characteristics of materials. For general energy, the ultra-soft pseudopotential technique is utilized. Ion potential is substituted with ultra-soft pseudopotential when using plane wave basis groups, which unfold the electronic wave function. Ions and electrons are included in the technology for ultra-soft pseudopotentials. The cut-off plane-wave energy is chosen at 571 eV for total-energy, band structure, and spectra computations. The exchange correlation potential is determined using two different approximations: the generalized gradient approximation (GGA) within the Perdew-Burke-Ernzerhof (PBE) function and the local density approximation (LDA) [27]. The Ultrasoft pseudopotential method is used for ion and electron interactions in this study, and the total energy convergence achieved is $1\times 10{-}5$ eV/atom. The limitedmemory Broyden-Fletcher-Goldfarb Shanno

(LBFGS) approach is a dependable technique for conducting a complete relaxation of lattice variables and interior coordinates to optimize the structure. The convergence parameters for maximum stress and displacement were imposed to 0.05 GPa and 0.001Å, respectively. Figure 1 depicts a cubic phase unit cell of Gd2O3 with four Gd 67 atoms and 18 O atoms, two nonequivalent Gd atoms at sites 8b and 24d, and one O atom at site 48e [28]. The electronic structure and optical characteristics of pure gadolinium oxide and Cd doped Gd2O3 were analyzed using a primitive cell. The Monkhorst-Park technique was applied to integrate the Brillouin zone, using a k-point mesh of 3*3*3 and cutoff energy is 571eV.

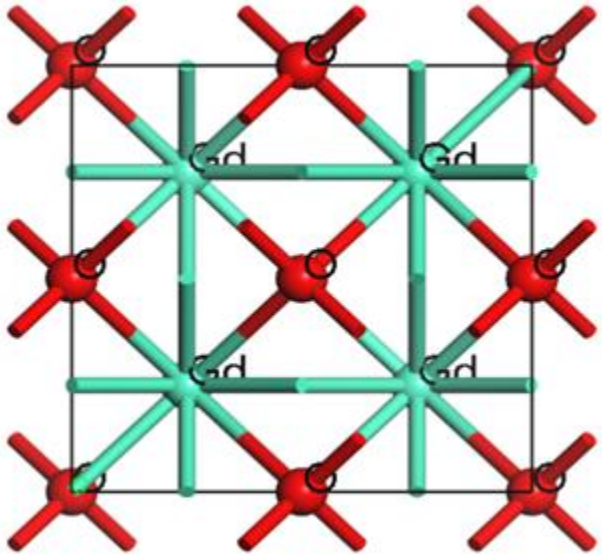

Figure 1 : Cubic structure of Gd2O3. The large and tiny spheres represent the atoms Gd and O, respectively.

In the current study, we have considered the configurations of Gd_2O_3 as Gd: $4f^7 5d^1 6s^2$ where [Xe] denotes core states and $(4f^7 5d^1 6s^2)$ valence states of Gd atoms, and O: $2s^2 2p^4$ where [He] represent core states and $(2s^2 2p^4)$ valence states of O atoms.

As we proceed, we create a Gd2O3 supercell with a scaling of (211) and examine the electronic characteristics such as band gap

and DOS by using DFT. After this, one Gd atom out of eight is replaced with Cd atom at super cellular level and recalculates the properties.

Results and Discussion

The unit cell of Gd_2O_3 was replicated to create a supercell with a 2*1*1 configuration which contains 39 atoms with 8 Gd and 31 O atoms, and a gadolinium atom was replaced by a cadmium atom in the crystal, which is known as cadmium doping as shown in Figure 2. Our goal is to examine the structural alteration and enhanced characteristics of Gd_2O_3 while doping the Cd at the super cellular level. We now have the modified band gap, DOS, and SCF calculations for this unit cell. When an atom of gadolinium in a Gd_2O_3 crystal is replaced by an atom of cadmium, it is called cadmium doping. The impact of cadmium doping on the features of gadolinium oxide depends on the concentration and distribution of the dopant atoms, as well as the specific properties being studied.

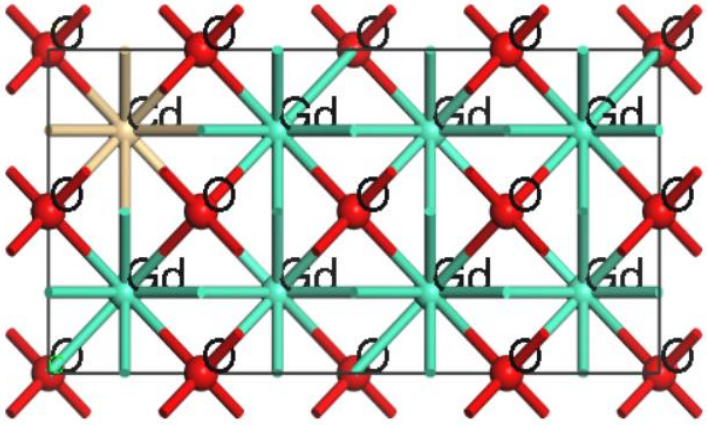

Figure 2: Crystal structure of 2 × 1 × 1 supercell of Cd-doped Gd_2O_3

For Cd-doped Gd_2O_3 structure with (space group Pn-3m), lattice parameters are a =10.715Å, b = c = 5.358Å, and cell angles are $\alpha=\beta=\gamma=90°$. Fine-quality pseudopotentials with energy cut-off of 250 electron volts (eV) were utilized to emulate the interaction

between the valence electrons and conduction holes in a precise manner for Cd-doped gadolinium oxide. By using an energy cut-off of 250 electron volts (eV), the calculations of band structure, density of states, electron density, and optical features were able to produce accurate and optimized results. To perform k-point grid sampling of reduced Brillouin zone using the Monhorst Pack scheme, a 3 × 3 × 3 grid was set for pure Gd_2O_3 while a 1 × 1 × 1 grid was used for Cd-doped Gd_2O_3. During the geometry optimization the energy convergence for this Cd-doped structure is 1.209 ×10−6 eV/atom, the highest displacement is 0.001Å, highest stress is 0.03 GPa, and highest force is 0.03 eV/Å. The total volume of lattice parameters is 307.589A^3. When Cd is introduced as a dopant in a material, the lattice parameters a, b, c, and the unit cell volume V are observed to increase. Additionally, the band gap Eg of the material is found to decrease with the incorporation of Cd dopants.

The impact of cadmium doping on the characteristics of gadolinium oxide can depend on concentration and distribution of the dopant atoms, as well as the specific properties being studied. In general, the introduction of a dopant atom can have several effects on the properties of a material, including changes in its electronic, optical, magnetic, and mechanical properties. Specifically, when a single atom of gadolinium in a Gd_2O_3 crystal is replaced by an atom of cadmium, the electronic and optical features of the material may be affected. For example, cadmium doping may introduce new electronic states into the material's band structure, which can alter its electronic conductivity, its optical absorption and emission properties, or its magnetic properties. Dopants can introduce new electronic states into the material's band structure, which can alter its electronic conductivity, optical absorption and emission properties, or magnetic properties. Dopants

can also create defects or distortions in the crystal lattice, which can affect the mechanical, thermal, or chemical stability of the material. Additionally, dopants can interact with other defects or impurities in the material, leading to further changes in its properties[29].

Electronic Properties of Pure and Cd-Doped Gd_2O_3 Crystal Structure

Band Structure of Pure and Cd-Doped Gd_2O_3 Crystal Structure

Analyzing the electronic properties of materials involve band structure and DOS, as these factors are significant in determining these properties. The calculated electronic band structure of un-doped Gd_2O_3 is presented in Figure 3a. In general, the band gap energy of the material is determined by the VBM and CBM, which are situated at G point in Brillouin zone. The energy scale is referenced to f*ermi level*, which has a position of 0 eV. The band gap of pure-Gd_2O_3, as determined by DFT-GGA calculations, is almost negligible small band gap [30].

In Figure 3 b, the electronic band structure for 2 × 1 × 1 supercell of Cd-doped Gd_2O_3 is depicted. The Cd dopant, which acts as an acceptor, results in addition to more bands in the structure with valence band is found to be convergent to the Fermi level. Gadolinium oxide has a band gap below zero i.e., the energy required to move an electron from valence band to the conduction band is extremely small. This means that the material can conduct electricity very easily, as the electrons in the valence band can easily move into the conduction band and flow through the material. Cadmium doping is responsible for modifying the electronic structure of the material and changing the position of the Fermi level, but it cannot fundamentally change the nature of the band gap. Doping with Cd, which is a group II element, has introduce additional energy levels into the

band gap and modify the electronic properties of the material, but it cannot eliminate the band gap entirely (see figure 3 b) [31].

Density of States (DOS) of Pure and Cd-Doped Gd_2O_3 Crystal Structure

In Figure 4 (a) & (b), total density of states (DOS) of pure and doped Gd_2O_3 crystal structure are presented. The DOS curves typically show two main regions: valence band and the conduction band. Valence band denotes the energy levels that are occupied by electrons in their ground state, while the conduction band denotes the energy levels that can be accessed by electrons when they are excited to higher energy states.

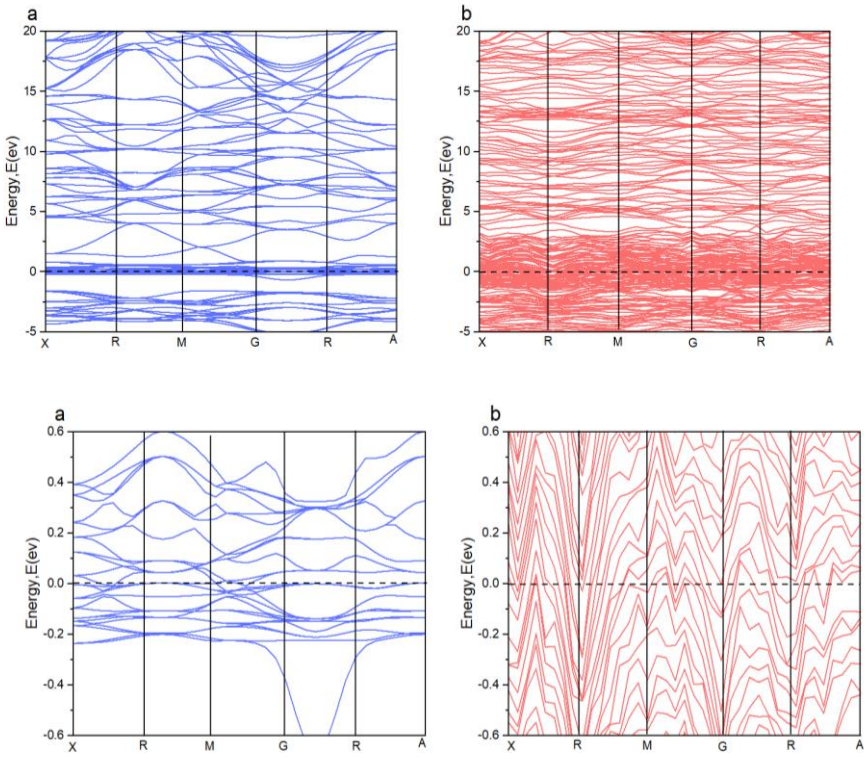

Figure 2: Band structure of (a) pure Gd_2O_3 and (b) Cd-doped Gd_2O_3

DFT calculations express that valence band of Gd_2O_3 is governed by oxygen 2p states, while the conduction band is dominated by gadolinium 5d states. The DOS in the valence band is relatively high and extends over a broad energy range, while the DOS in the conduction band is lower and more sharply peaked. Results show that Band gap of gadolinium oxide (Gd_2O_3) is zero, and then its density of states (DOS) curve would show a continuous distribution of electronic states across the entire energy range. In other words, there would be no energy gap between the valence and conduction bands, and DOS would be non-zero at all energies. In such a scenario, there would be no energy gap between valence and conduction bands, and there would be available electronic states at all energies [32].

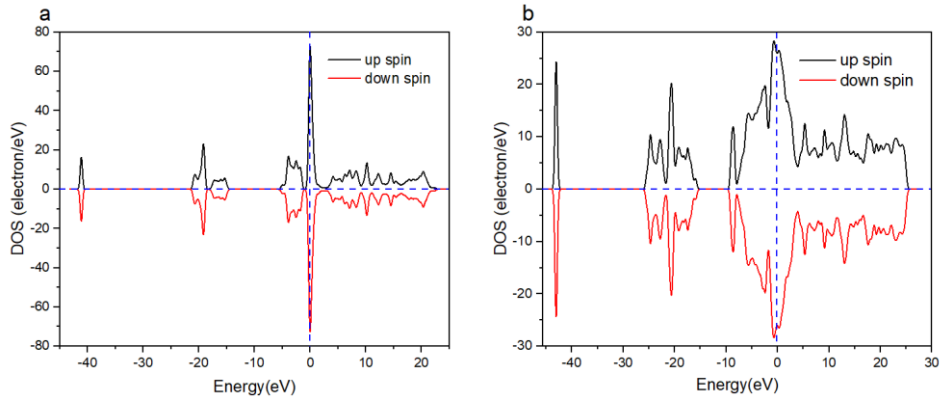

Figure 4: Calculated total density of states of (a) pure-Gd_2O_3 and (b) Cd-doped Gd_2O_3 in 2 × 1 × 1 supercell.

As seen in figure most frequently, the O-$2s$ and Gd-$5p$ states are found between -20 and -15eV. O-2p and Gd-5d states arise as bands in the energy ranges of around 3.3 eV to 0 eV, with overall widths of about 3.25 and 3.3 eV, respectively. The Gd-5d state also shows out near the bottom of conduction band. In DOS, Fermi level is taken to be 0 eV. After doping

peaks for Cd up and down spin occur at an energy of -9 eV, and band structure of Cd doped Gd_2O_3 tends to narrow down with more heavily populated with electronic states as depicted by DOS (see figure 4b). This is because doping with Cd, which is a group II element, has introduced additional energy levels into the band gap and modified the electronic properties of the Gd_2O_3 , but it cannot eliminate the band gap entirely.

Conclusion

In this study, we investigated the structural and electronic characteristics of cubic Gd_2O_3 within a density functional theory framework. Calculations demonstrate that there is a direct band gap in the gamma direction and structural optimizations were carried out with acceptable accuracy. Furthermore, Cd doping has a significant effect on the band structure and density of DOS with increasing the population of energy states of valance band. The results reported in this study are significant for optoelectronics applications in replacement cadmium for reduce the cytotoxicity issues associated with it.

References

1. Zatsepin, D., et al., *Electronic structure, charge transfer, and intrinsic luminescence of gadolinium oxide nanoparticles: Experiment and theory.* Applied Surface Science, 2018. **436**: p. 697-707.
2. Geoffrey N áCloke, F., *Zero oxidation state compounds of scandium, yttrium, and the lanthanides.* Chemical Society Reviews, 1993. **22**(1): p. 17-24.
3. Hong, M., et al., *Epitaxial cubic gadolinium oxide as a dielectric for gallium arsenide passivation.* Science, 1999. **283**(5409): p. 1897-1900.
4. Chaubey, N., et al., *Physicochemical properties of rare earth doped ceria Ce0. 9Ln0. 1O1. 95 (Ln= Nd, Sm, Gd) as an electrolyte material for IT-SOFC/SOEC.* Solid state sciences, 2013. **20**: p. 135-141.

5. Lu, Y., et al., *Efficient ion conductivity enhancement mechanism induced by metal ion diffusion of SOFCs based on Fe-doped Gd2O3 electrolyte.* Electrochimica Acta, 2023. **458**: p. 142481.
6. Wang, C., *Solid Electrolytes Based on Rare Earth Oxides and Fluorides*, in *Theory and Application of Rare Earth Materials*. 2023, Springer. p. 91-107.
7. Shlyakhtina, A., et al., *Proton/oxygen ion conductivity ratio of Nd containing La10W2O21/γ-La6W2O15 tungstates.* International Journal of Hydrogen Energy, 2023.
8. Salek, G., et al., *Tuning the composition of rare earth sesquioxides Gd 2− x La x O 3: Eu 3+ to control phase transitions at a high temperature to design new highly sensitive luminescence-based thermal sensors.* RSC Advances, 2016. **6**(60): p. 55298-55306.
9. Li, S., *Unveiling the structure and reactivity of rare earth oxides and gold catalysts through density functional theory*. 2023, Universität Bremen.
10. Khan, M.M. and S.N. Matussin, *Sm 2 O 3 and Sm 2 O 3-based nanostructures for photocatalysis, sensors, CO conversion, and biological applications.* Catalysis Science & Technology, 2023. **13**(8): p. 2274-2290.
11. Sammes, N. and Y. Du, *Intermediate-temperature SOFC electrolytes*, in *Fuel Cell technologies: state and perspectives*. 2005, Springer. p. 19-34.
12. Eyring, L., *The binary rare earth oxides.* Handbook on the physics and chemistry of rare earths, 1979. **3**: p. 337-399.
13. Xia, X., W. Hu, and Y. Shao, *Density functional theory calculations for the structural, electronic, and magnetic properties of (Gd2O3) n 0,±1 Clusters with n= 1–10.* The Journal of Physical Chemistry C, 2015. **119**(15): p. 8349-8356.
14. Gursal, S.A., et al., *Investigating the effect of adding CdO nano particles on neutron shielding efficacy of HDPE.* Radiation Physics and Chemistry, 2020. **177**: p. 109145.
15. Rehman, M.S.U., et al., *Investigation of Metal Oxide Nanoparticles by*

Using Punica granatum Extract. NUST Journal of Natural Sciences, 2021. **6**(1).

16. Minhas, A.S., et al., *Phytochemical Investigation, Synthesis and Characterization of Iron Oxide Nanoparticles by Peel Extract of Punica Granatum.* NUST Journal of Natural Sciences, 2021. **6**(2).
17. Irfan, A., et al., *A Potential Approach to Enhance the Seebeck Coefficient of UHMWPE by Using the Graphene Oxide.* Non-Metallic Material Science, 2020. **2**(2): p. 21-27.
18. Saeed, M.M., et al., *Diffuse reflectance spectroscopy of γ-irradiated UHMWPE: A novel fractional order based filters approach for accessing the radiation modification.* Radiation Physics and Chemistry, 2022. **197**: p. 110163.
19. Mehmood, M.S., et al., *Mueller matrix polarimetry for characterization of E-Beam irradiated Uhmwpe.* Radiation Physics and Chemistry, 2020. **166**: p. 108503.
20. Gursal, S.A., et al., *On the neutron shielding efficacy of flexible silicone infused with CdO nanoparticles.* Radiation Physics and Chemistry, 2023. **202**: p. 110555.
21. Mehmood, M., Y. Khan, and T. Yasin, *Optical properties of UHMWPE-II: Photon distributions studies using Monte Carlo simulation.* Radiation Physics and Chemistry, 2019. **158**: p. 103-108.
22. Mehmood, M.S., et al., *UHMWPE band-gap properties-II: Effect of post e-beam irradiation real time shelf aging in air.* Radiation Physics and Chemistry, 2019. **159**: p. 231-237.
23. Mehmood, M.S., et al., *Assessment of γ-sterilization and/or cross linking effects on orthopedic biomaterial using optical diffuse reflectance spectroscopy.* Optik, 2017. **144**: p. 387-392.
24. Rizwan, A., et al., *Simulation of light distribution in Gamma Irradiated UHMWPE using Monte Carlo model for light (MCML) Transport in Turbid Media: analysis for industrial scale biomaterial Modifications.* Polymers, 2021. **13**(18): p. 3039.
25. Ullrich, C., *Density functional theory.* Bulletin of the American Physical Society, 2023.

26. Hermet, J., et al., *Thermodynamics of hydration and oxidation in the proton conductor Gd-doped barium cerate from density functional theory calculations.* Physical review B, 2012. **85**(20): p. 205137.
27. Mondal, A.K., et al., *First-principles studies for electronic structure and optical properties of p-type calcium doped α-Ga2O3.* Materials, 2021. **14**(3): p. 604.
28. Perevalov, T.V., et al., *Atomic and electronic structure of gadolinium oxide.* The European Physical Journal-Applied Physics, 2014. **65**(1).
29. Mondal, A., et al., *First-Principles Studies for Electronic Structure and Optical Properties of p-Type Calcium Doped α-Ga2O3. Materials 2021, 14, 604*. 2021, s Note: MDPI stays neutral with regard to jurisdictional claims in published ….
30. Yao, G., et al., *Electronic and optical properties of Rocksalt CdO: a first-principles density-functional theory study*. Model Numer Simul Mater Sci, 2013. **3**: p. 16-19.
31. Ambrosch-Draxl, C. and J.O. Sofo, *Linear optical properties of solids within the full-potential linearized augmented planewave method.* Computer physics communications, 2006. **175**(1): p. 1-14.
32. Zhang, F., et al., *Structural phase transitions of cubic Gd 2 O 3 at high pressures.* Physical review B, 2008. **78**(6): p. 064114.